THE CONCEPTUAL DESIGN OF THE RHIC RF SYSTEM

RHIC Project
Brookhaven National Laboratories
Upton, NY 11973-5000

September 20, 1994

Contents

List of Figures

List of Tables

Chapter 1

INTRODUCTION

The Relativistic Heavy Ion Collider complex at Brookhaven consists of two rings in which counter-rotating beams of particles collide head-on at up to six interaction regions. The machine consists of superconducting magnets together with room temperature equipment located in various warm regions of the rings. The facility is designed to collide various species of fully stripped ions ranging from the lightest, protons, to gold ions, in an energy range of up to 250 GeV for protons, 100 GeV/u for gold ions. The major machine parameters are listed in Table 1.1. A primary accelerator sub-system is the rf system. This report details the conceptual design of this system together with the technical issues which are relevant to this design.

Circumference (m)	3833.852
Average radius (m)	610.176
Revolution frequency (kHz) $(v = c)$	78.196
Transition energy γ_{tr}	22.8
Bunches/ring	57 (114)
Horizontal tune (ν_x)	28.19
Vertical tune (ν_y)	29.18
Transverse emittance (95%) $(\pi mm\text{-}mrad)$	10 to 40
Longitudinal emittance (Au) (eVs/u)	0.2 to 0.4 to 1.2
Longitudinal emittance (p) (eVs)	0.3 to 0.33
Maximum dispersion (m)	1.84
Maximum dispersion with γ_{tr}-jump (m)	1.84
Magnetic rigidity (injection) (Tm)	96.7
Magnetic rigidity (top) (Tm)	839

Table 1.1: *RHIC* machine parameters

The *RHIC* rf system must capture 57 (114 in future upgrade) bunches each injected individually from the *AGS* , damp the bunch to bunch injection errors, accelerate them to top energy, and store the beam for 10 hours. Particle species vary from protons to fully stripped gold with all ions except protons going through transition. The varying requirements this imposes on the rf are satisfied by three systems:

- An accelerating system (26MHz system) for capture of the injected beam, acceleration to top energy, and bunch shortening at top energy.

- A storage system (196MHz) for provision of sufficient longitudinal focusing to keep bunches short during the 10 hour storage time.
- A longitudinal kicker to damp longitudinal injection errors of individual bunches and for damping longitudinal coupled bunch instabilities.

Systems	Accelerating	Storage	Kicker
Harmonic	342	2508	
Radio frequency (MHz)	26.743	196.12	wide band
Stations	4	10	2
Stations/ring	2	3+4	1
Voltage/station (kV)	300	1000	1
Voltage/ring (kV)	2×300	7×1000	1×1

Table 1.2: Total *RHIC* cavity systems and longitudinal kicker.

Table 1.2 lists the major characteristics of these system. Figure 1.1 shows the rf cavity layout in the 4 o'clock intersecting region of the *RHIC* enclosure. Two accelerating cavities are located in the 40 m warm region between magnets Q3 and Q4. The 0.9 m horizontal ring separation requires staggering the cavities in the two rings. The ten storage cavities are divided with four cavities common to both rings close to the interaction point and three each per ring adjacent to the accelerating systems. This configuration allows the common cavities to provide voltage to both rings at the same time, reducing the overall number of cavities needed.

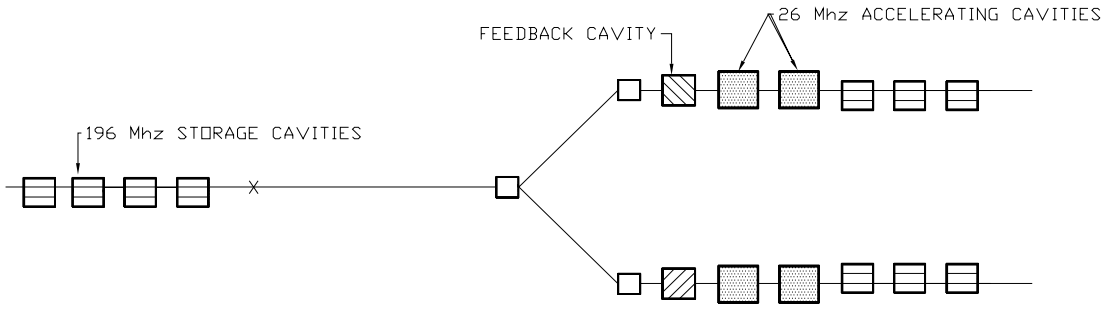

Figure 1.1: Schematic layout of the 4 o'clock interaction region showing the positioning of rf cavities.

The machine cycle can be divided into several critical areas with different problems and requirements: injection, acceleration, transition crossing, beam transfer from the low frequency to the high frequency system and storage. An important step for the beam manipulations is the transfer from the accelerating system to the storage one (rebucketing). Excessive emittance growth prior to this point in the cycle can lead this operation to cause beam loss and possible magnet quenching.

The *AGS* will provide bunch to bucket injection of ions from protons through Au. For proton bunches a bunch rotation in the *AGS* is used before extraction to allow a higher matching voltage in *RHIC* . Gold bunches are directly injected into *RHIC* . The voltage is then increased to the nominal accelerating voltage from the matching voltage as the magnet ramp begins and the beam is accelerated (through transition for all ions except protons) to top energy. The slow 500 gauss/sec ramp of the superconducting magnets would produce a large emittance growth and beam loss during the transition crossing time so a γ_{tr}-jump is used to reduce this crossing time to 60 milliseconds. In order to transfer the gold beam from the accelerating system into the shorter buckets of the storage system a bunch rotation is used to shorten the nominally 7.5 ns long bunches to 4 ns (280 degrees of the bucket). The accelerating system is then turned off and the storage system voltage increased to the matching voltage. After capture the storage voltage is increased rapidly to its maximum value to provide maximum integrated luminosity during the 10 hour storage. During storage for the heaviest ions at design intensities, intra-beam scattering is estimated to cause rapid emittance growth in both transverse and longitudinal planes resulting in a completely filled bucket and continuous beam losses. The basic bunch parameters are shown in Table 1.3 for the two extreme ion species (protons and gold).

	P (inj)	P (top)	Au (inj)	Au (top)
Bunch length (ns)	6.5	4	13.5	7.5
Synchrotron frequency (Hz)	45	25	90	27
Charge state (Z)	1	1	79	79
Bunch area (eVs/u)	0.3	0.33	0.2	0.4
Normalized emittance ($\pi mm\text{-}mrad$, 95%)	20	20	10	15
Number of ions per bunch	10^{11}	10^{11}	10^{9}	10^{9}
Energy (γ)	31.2	268.4	12.6	108.4

Table 1.3: Bunch parameters

The balance of this report examines each step in the proposed machine cycle, details the issues involved and explains the logic for the design choices and associated system parameters. The operating cycle is defined and hardware details are discussed.

Chapter 2

INJECTION

Bunches of particles are loaded into the *RHIC* rings in box car fashion from the *AGS* injecting into matched stationary buckets. One bunch is extracted from *AGS* at a time and can be injected into any preselected bucket in *RHIC* . In this way the limitation on which harmonic that *AGS* has to run is lifted, which makes *AGS* more flexible for *RF* gymnastics. If more than one bunch is extracted and injected into *RHIC* , then the bunch separation remains in both machines. Therefore, *AGS* has to run at a harmonic constrained by the harmonic of *RHIC* , the ratio of two machines' circumferences and the *RF* frequencies. For example, given that *RHIC* is running at harmonic 342 and 26MHz, at extraction *AGS* has to run a harmonic of 12 and $\frac{1}{6}$ of *RHIC* frequency.

The time delay between successive bunches of the same batch injected is determined by the recharge time of the injection kickers and is estimated to be ~ 30 ms. The filling time is about ~ 1 minute for both rings. It is important to keep this filling time relatively short for gold ions since at these energies the intra-beam scattering growth time is rapid for the gold ions ($\tau \sim 6$ min) and dynamic aperture effects in the 8 cm magnets are worst at injection energies due to the large physical beam size. The storage rf system is not used at all during this process and to minimize the potential effects of beam loading in these devices a system of cavity dampers will be inserted into the elements.

There are three operating scenarios to consider which cover all other cases:

- gold on gold
- proton on proton
- proton on gold

For the first two scenarios, we shall alternatively load one batch of bunches into one ring and the next batch of bunches into the other ring; then accelerate both beams to the operational energies. This alternate ring transfer serves to equalize the average dwell time for the bunches in both rings resulting in more uniform bunch parameters. In the scenario of protons on gold, since the intra-beam-scattering causes significant beam emittance blowup for gold ions and the time to switch from one ion species to another in the injector is not known in detail, we shall fill one ring with the proton beam first, and then fill the other with heavy ions. Both beams are then accelerated to the collision energy.

Emittance dilution due to injection phase and energy errors is expected and we have assigned a tolerance of 10% dilution from the transfer process itself as the goal. In addition to a systematic emittance growth, we also expect a random bunch to bunch emittance variation of an additional 10% base on *AGS* operating experience for heavy ions [1]. During the injection process some bunches will experience up to a ~ 1 min

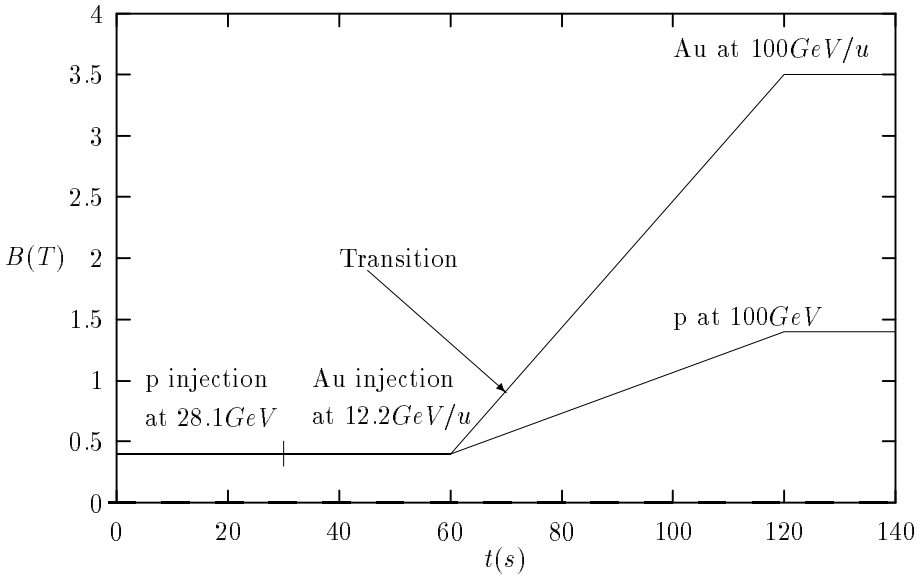

Figure 2.1: Injection scenario for protons on gold ions.

dwell. This will result in a further emittance variation of up to $\sim$ 20% between the first and last bunches for gold ions.

2.1 Synchronization and Cogging

Synchronization and cogging are the two steps involved in transferring a bunch from *AGS* into a predetermined bucket in *RHIC* at the proper phase. Synchronization matches the phases of the bunch and the bucket, after synchronization cogging simultaneously aligns the bunch to the extraction kicker and the bucket to the injection kicker and triggers both kickers (a constant time delay between these two kickers). Since many batches of bunches are needed to fill *RHIC* , both processes derive their reference signal from *RHIC* buckets (cavity sum voltage) which are fixed due to already injected bunches. The *RHIC* rf voltage signal is taken and downgraded by an integer number to phase lock with *AGS* rf signal, synchronization and cogging can then be followed.

The cogging process triggers the extraction and injection kickers, and thus determines the filling pattern of bunches into *RHIC* . Let's focus on filling one ring. This is done by two state machines. The first state machine keeps track of the *RHIC* buckets and thus has 342 states and the name of bucket state machine. When the bucket state machine is started, it goes to state one and advances one state after each rf period. The second state machine has 342 branches, each of which corresponds to a bucket and has two states 1 and 2. The connections among these branches determined the filling pattern, it is therefore referred as the bunch state machine. For example, buckets $i\ j\ k$ are to be filled successively. After a trigger is sent to the kickers and thus bucket i is filled, the bunch state machine goes from the ith branch to state 1 in the jth branch and waits there for a ready trigger. When the ready trigger has arrived, it goes to the state 2 and wait there. Once the bucket state machine reaches state j, it sends out a trigger to the kickers and moves on to branch k. The bunch state machine needs to be programmable and down-loadable.

2.2 Voltage Matching

To eliminate potential longitudinal emittance blowup, the accelerating cavity system has to create stationary buckets to match the shape of incoming bunches. There is no specific allocation for emittance dilution arising from mismatched buckets. The major system parameters at injection are listed in Table 2.1 for gold ions.

Kinetic energy (GeV/u	10.4
Matching rf voltage (kV)	170
Bucket area (eVs/u)	0.88
Bunch area (eVs/u)	0.2
Bucket width (ns)	37.5
Bunch width (ns)	13.5
synchrotron frequency (Hz)	90

Table 2.1: Major parameters for gold beam at injection.

For the proton beam the proximity between transition and injection energies results in a nominal matching voltage of only $\sim 19kV$ [2]. Since the beam induced voltage in a accelerating cavity is $\sim 12kV$, for the nominal bunch intensities, then maintaining a matched voltage in the presence of a proportionally very large transient effect is difficult to achieve. Gold ions with a matching voltage of 179 kV are much less sensitive to this effect. Reducing the bunch length by a factor of 1.8 in AGS by means of a bunch of rotation prior to transferring the bunch will raise the matching voltage by a factor of 10 (1.8^4), thus avoiding the complications of running at very low voltages. For this reason this scheme is taken as the nominal operating cycle for the protons and results in system parameters as given in Table 2.2.

Kinetic energy (GeV/u	28.1
Matching rf voltage (kV)	196
Bucket area (eVs/u)	5.2
Bunch area (eVs/u)	0.3
Bucket width (ns)	37.5
Bunch width (ns)	6.5
synchrotron frequency (Hz)	45

Table 2.2: Major parameters for proton beam at injection.

An alternate possibility that does not involve gymnastics in the AGS is to obtain the low voltages required by counter-phasing the two cavities in a way that the voltage vector sum is much smaller than the two individual voltages (i.e. each cavity is at 200 kV, but the total sum is 50 kV). In this case phase noise can set a lower limit on the minimum achievable effective voltage. Assuming that phase noise of $sim0.5$ degrees is achieved in the electronics, than it can be shown that the cavities must be run at a maximum 60 kV each to yield a total vector sum of 20kV with less than 5% of amplitude ripple [3].

Using a single bunch loading scheme, there are periods during the injection time where the $RHIC$ ring is partially full. The beam induced voltage developed on the accelerating cavities by a partially filled ring reaches a maximum of 4kV when the ring is half filled. This transient voltage is in phase with the beam

image current and in quadrature with the required gap voltage. The pas shift due to this voltage is less than 2 degrees. Uncorrected, this will lead to a small mount of emittance growth, but a phase error of this amount can be corrected by the wide band damper.

2.3 Longitudinal Damping

Since longitudinal injection errors are inevitable and these errors are generally different for different bunches, it is necessary to have a wide band cavity (bandwidth $\geq \pm 57 f_0$, where f_0 is the revolution frequency in the *RHIC* ring) capable of bunch-to-bunch damping of such errors and also providing control of coupled-bunch coherent instabilities.

Assuming some fixed longitudinal error at injection, the damper power required is inversely proportional to how much emittance growth we want to allow. We have chosen a 10% emittance growth allocation for bunch to bunch random injection errors (systematic errors are assumed to be small compared to these). In the absence of any damping mechanism then the estimated momentum error of $l0^{-4}$ would result in a 30% emittance dilution of a $0.2eVs/u$ bunch. the required damping time is defined by the decoherence time arising form synchrotron frequency spread in the bunch. For the case of gold ions this is $\sim$ 100 ms or about 10 synchrotron periods. Several studies of an injection damping system have been made: E. Raka [1] found for linear feedback the maximum voltage required is 700V. J. Xu [4] studied the coherent motion of a bunch under a longitudinal kicker, he found a maximum of 400Vis needed to damp the initial error in the decoherence period with a constant voltage mode in which the damper provides a constant kicking voltage. D-P Deng [5] studied how much emittance blowup occurred at the end of injection error damping. For a kicking voltage of 1000V per turn, approximately 10% emittance growth is expected in the decoherence time assuming linear damping. Requiring less that 5% emittance blowup increases the necessary voltage to well over 7000V. Hardware considerations indicated that a 700V system with an effective bandwidth of 30 MHz is a reasonable compromise between emittance growth on one haven and cost and complexity on the other, and these are the baseline parameters chosen for the damping system. A damper with these parameters is capable of damping coupled bunch growth rates of up to 10^{-1} [1].

2.4 Coupled Bunch Instabilities

The growth rates of coupled bunch instabilities due to the high order modes in the accelerating and storage cavities have been calculated both analytically and numerically.

For a bunch distribution in the longitudinal phase space given by:

$$\Phi(r) = K(1 - (\frac{r}{r_\phi})^2)^{\frac{3}{2}} \tag{2.1}$$

where K is a normalization constant, then the growth rate of coherent oscillations driven by an effective narrow band cavity is [6]:

$$\frac{1}{\tau_m} = \frac{\omega_\nu I_0 R}{r_\phi V_{rf} \cos\phi_s} F_m \tag{2.2}$$

where m is the mode number (m=1,2... are the dipole, quadrupole ... modes), I_0 is the DC current of the bunches, R is the impedance of the cavity, ω_v is the angular synchrotron frequency, r_ϕ is the bunch half length measured in radians i the fundamental mode, and Fm is a form factor which has been found analytically by K. Satoh [7] as a function of the mode and bunch distribution and is always less than 0.6.

The Higher Order Mode (HOM's) structures of the 26.7 MHz and 196.1 MHz cavities were calculated with the code URMEL. The code calculates frequency (f_{res}), shunt impedance (R_{sh}) and quality factor (Q) assuming axisymmetric cavities. Although the values calculated are accurate to within a few percent for most HOM's, this is not sufficient for the frequency resolution required for couple bunch mode analysis which requires frequency resolution required for coupled bunch mode analysis which requires frequency resolution better than the revolution frequency, in this case 78 kHz. Even if the frequency calculation was exact, the HOM's in the accelerating cavity can be expected to be tuned along with the fundamental 26.7 MHz mode which must be tuned 0.35% to compensate for the velocity increase of the beam during acceleration. Applying this to a 100 MHz HOM results in a 350 kHz shift, which would tune it over several revolution lines. Therefore the worst cast of cavity resonances lining up with rotation lines was taken in the coupled bunch instability analysis to determine worst case growth rates. The data in Table 2.3 are the calculated f_{res}, R_{sh} and Q of the 26.7 MHz accelerating cavity for *RHIC* . The 196.1 MHz cavities are modified SWC cavities which have HOM suppressors already designed. The data in Table 2.4 shows the calculated HOM frequencies of the modified CERN cavities (fundamental $f_{res} = 196.1MHz$) with the R_{sh} and Q's of the unmodified cavity with mode suppressors. Since no hardware measurements have been made yet, these are the calculated (undamped) values from URMEL. Since the HOM dampers on the CERN cavities are broadband, changing the frequencies of the modes should not to first order change the damped or undamped R's and Q's. Although cavity modifications may alter the mode spectrum, these values should be representative of the final design.

f_{res} (MHz)	R_{sh} $(M\Omega)$	Q	Au growth rates/mode (s^{-1})	P growth rates/mode (s^{-1})
26.8	0.930	12000	na	na
64.8	0.038	15300	2.838	6.731
119.3	0.04	27400	0.146	3.944

Table 2.3: *RHIC* accelerating cavity mode structure and coupled bunch growth rates.

f_{res} (MHz)	R_{sh} $(M\Omega)$	Q	Au growth rates/mode (s^{-1})	P growth rates/mode (s^{-1})
196.1	0.0178	94	$<< 0.1$	0.60
308.4	0.0704	4400	2.838	0.11131
445.0	0.01	1200	$<<0.1$	$<<0.1$

Table 2.4: *RHIC* storage cavity mode structure (damped) and coupled bunch growth rates.

Using these HOM data, numerical calculations of longitudinal coupled bunch instability thresholds and growth rates have been made for both protons and fold. The Sacherer formalism with 57 identical bunches, and without synchrotron mode coupling, was used to model the beam. The impedance assumed consisted of the rf cavity modes from Tables 2.3 and 2.4, space charge ($Z/n = i5\Omega$ for gold, $i1\Omega$ for protons at injection) and a broad band component due to bellows etc. ($Z/n = -i2\Omega$). Growth rates are determined by the real part of the impedance which is dominated by the parasitic cavity modes. For an undamped cavity system we estimate that the growth rates should be nor more that $20s^{-}1$. We are assuming that HOM damping can reduce the offending modes by a factor of 10, which in turn would reduce these growth rates by an equivalent amount. The resulting growth rate of $2s^{-1}$ is well within the longitudinal damper capability of $10s^{-1}$ if not Landau damped. The magnitude of the frequency shifts are the major factors in determining

the stability of the beam, and are determined by space charge and the broad band impedance at injection energies. On the basis of this analysis the beams appear to be stable with the 64 MHz and 119 MHz modes of the accelerating cavities requiring some form of mode damping for proton operation.

Chapter 3

ACCELERATION

The nominal acceleration ramp takes 1 minute and is determined by the available power supply voltage. All ion species cross transition at an energy of $\gamma_{tr} = 22.8$, except for protons.

Two topics are addressed in detail below - the synchrotron frequency crossing harmonics of the 60 Hz power line, and derivation of the specifications for the acceleration cavity tuners. Both of these depend directly on the nominal acceleration ramp parameters that are needed for different species in the Chapter 7: Operating Cycle.

3.1 Power Line Harmonic Crossing

If gold ions are accelerated with a constant acceleration voltage of 300 kV, the small amplitude synchrotron frequency f_ν drops rapidly from about 90 Hz to 0 Hz at transition, and then rises to a local maximum at about 35 Hz, before settling at about 27 Hz prior to transfer to the storage system (when f_ν becomes about 300 Hz) [2]. On the other hand, protons accelerated with 300 kV encounter a synchrotron frequency that swings smoothly between about 45 Hz and 25 Hz, without crossing transition. In both cases the longitudinal dynamics are vulnerable to resonances caused by voltage and phase modulation at harmonics of the line frequency. For example, voltage modulation at a frequency

$$f_m = k \ 60 \ \text{ Hz}$$

potentially creates a chain of resonance islands inside the rf bucket, at synchrotron frequencies given by

$$f_s = \frac{n}{2} f_m$$

where n is the integer index of the resonance [8]. The strongest noise peak is (presumably) at $k = 1$, and the strongest resonant response is for $n = 1$, showing that ions are most vulnerable when f_ν crosses 30 Hz. If the synchrotron frequency passes slowly through 30 Hz, ions are resonantly trapped, leading to emittance blowup.

The synchrotron frequency of a test particle, f_s, drops from f_ν to about 0.75 f_ν as its relative amplitude a_s rises from zero to 0.75 - three quarters of the way to bucket separatrix. In order to deny resonances the possibility of becoming adiabatically stable for $a_s \leq 0.75$, it is therefore necessary to pass quickly through the region

$$30 \ \text{ Hz} \ < f_{s0} < 40 \ \text{ Hz}$$

It can be shown [8] that the rapid transit condition for non-adiabaticity is

$$\frac{|df_\nu|}{dt} > \frac{\pi}{2}\epsilon\ a_s^2 \frac{f_\nu^3}{f_m}$$

where ϵ is the depth of the voltage modulation. For example, if $\epsilon = 10^{-3}$ (large), $a_s = 0.75$, $f_s = 30$ Hz, and $f_m = 60$ Hz, then the dangerous region of 30-40 Hz should be passed at a rate faster than about 0.4 Hz per second. This rule is (only just) obeyed by the nominal constant voltage proton acceleration ramp. The voltage in the nominal gold acceleration ramp is lowered from 300 kV to 170 kV, just after transition, to avoid this effect and keep the synchrotron frequency less than 30 Hz. The voltage is returned to 300 kV just before the end of the acceleration ramp.

3.2 Acceleration Cavity Tuner Specification

We need to tune the 26 MHz acceleration system to accommodate changes in the beam revolution frequency during acceleration, and to compensate for beam loading. The beam loading detune is rather small and has negligible impact on the tuner design, the bulk of the tuning goes into synchronizing with the beam acceleration.

The detuning required for beam loading compensation is given by

$$\Delta f_{rf} = \pm \frac{I_0 \cos(\phi_s)}{V_{rf}} \frac{R}{Q} f_{rf}$$

where ϕ_s is the synchronous angle, I_0 is the average beam current, a value of $R/Q = 69$ is expected for these cavities, and the sign of the shift is positive below transition and negative above. Since the relative low beam intensity and high rf voltage, this frequency change is always less than 1 kHz for *RHIC* parameters.

Gold ions are accelerated from $\gamma = 12.6$ to $\gamma = 108.4$, while protons are accelerated from $\gamma = 31.2$ to $\gamma = 268.4$. The rf frequency is given by

$$f_{rf} = \frac{hc}{C}\sqrt{1 - \frac{1}{\gamma^2}}$$

where c is the speed of light, C is the *RHIC* circumference, and h is 342 , the harmonic number. Take the limit of the speed of light the rf frequency is 26.743 MHz. Gold ions are slowest at injection, which gives rise of the rf frequency of 26.658 MHz. So the frequency range required on this basis is 85 kHz.

Therefore 0.5% tuning range, which is roughly 125 kHz, should be sufficient. The fastest rate of change of rf frequency is about 23 kHz per second, for gold ions at the beginning of the acceleration ramp. This sets the specification for the response speed of the tuner.

Two different tuner designs are currently under study. One employs perpendicularly biased ferrites, which are enclosed in a fast tuning loop. The other, more conservative, design is for a mechanical tuner that changes the dimensions of the accelerating gap. Thanks to the relatively slow ramp rate of the superconducting magnets, the stepper motor controlling this tuner does not need to be especially fast. n The accuracy with which the rf phase can be controlled has been calculated as a function of the stepper resolution, using preliminary design parameters [9]. Emittance growth has been calculated to be less than 1% if the phase error is kept less than 0.23 degrees [10]. With beam control feedback of a factor of 100, the allowable phase error becomes 23 degrees which is easily satisfied. The amplitude step resolution is approximately the sum of the total ring voltage of either the acceleration or the storage system, divided by 16 bits, to become 2×300 kV$/2^{16} = 9$ Volts or 8.1 MV$/2^{16} = 120$ Volts, respectively.

The two tuner designs will be evaluated when they are complete, and one will be chosen for use. The specifications outlined above are not difficult to meet with either type of tuner.

Chapter 4

TRANSITION CROSSING

This section summarizes the various longitudinal problems associated with crossing transition energy. With the exception of protons, all other ions will cross transition. The RHIC facility is unique in the fact that emittance dilution at transition can cause the subsequent transfer to the storage system to be lossy and inefficient, while beam losses themselves at transition or later in the cycle can lead to magnet quenching. Systematic beam loss at any point in the cycle of a superconducting machine can easily produce severe operational consequences. RHIC will be the first superconducting machine to cross transition energy. At a fixed value of the synchronous phase, as transition approaches, the bunch energy spread expands while the bunches become very narrow in the time extent. The large energy spread alone can cause problems if it forces particles outside of the available momentum aperture. Particle dynamics are influenced by transition effects during a time scale where the particle motion in non-adiabatic [11]. The inherently slow acceleration rate of a superconducting machine produces a correspondingly long non- adiabatic time, 100 ms at RHIC, which results in much more severe effects than observed at rapid cycling conventional accelerators.

Beam loss and bunch area growth can be caused by both single and multi-particle effects. In the former category are chromatic non-linear effects produced by particles of different momenta crossing transition energy at different times. The most important multi-particle effects are due to the changing sign of the space charge component of the bunch at transition, producing a bunch shape mis-match to the bucket and potential microwave instabilities during the narrow bunch regime. These effects have been investigated both analytically and numerically [11] with good agreement between the two techniques. The results of these studies show that in the absence of any preventative measures then for the nominal beam parameters for Au ions (10^9 ppb, $0.3eVs/u$) a beam loss of up to 70% could be anticipated. The solution to this situation is the use of a transition (γ_{tr}) energy jump. An analysis of the jump parameters obtained primarily from numerical studies [12] show that a clean crossing (10% emittance dilution, no beam loss) is obtained with a γ_{tr}-jump of 0.8 units within a time period of 60ms. Features of this analysis include the need to control the beam induced parasitic voltage in the storage cavities to 10kV during this time, and a relatively narrow window on longitudinal emittance around the design value of $0.3eVs/u$ where the emittance can be preserved even with a γ_{tr}-jump. The estimated relationship between initial and final longitudinal emittance is shown in Figure 4.1 At nominal bunch intensity, space charge induced emittance growth is present for smaller initial emittances and chromatic non-linearities result in emittance growth for values greater than $0.3eVs/u$. In view of this sensitivity of the jump dynamics to initial parameters then the bunch emittance variation becomes a critical factor in a loss free (or dilution) transition jump. The two main factors contributing to bunch to bunch emittance spread are the rapid IBS growth time at injection energy where some bunches are forced to survive up to 60s before acceleration, and the natural cycle to cycle emittance variation of the

injector. Systematic emittance growth of 20% is estimated for the first bunches injected. Bunch to bunch variation arising from the injector chain can also be expected to contribute an additional 10%, together with another 10% arising from bunch to bunch energy - phase errors. Since efficient rebucketing requires a final emittance of no greater than $0.4eVs/u$ then the injector is required to provide a nominal emittance of $0.2eVs/u$ at extraction. The proposed emittance evolution is given in Table 7.1 in section VII.

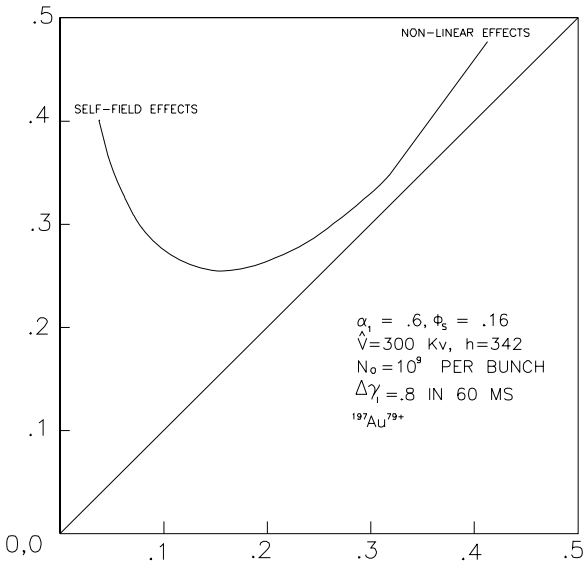

Figure 4.1: Initial versus final longitudinal emittances (eVs/u) with a 60 ms transition jump.

A γ_{tr}-jump has thus been incorporated into the machine design. The balance of this section describes the lattice design of the jump, beam loading considerations, the hardware implications of transition on the RF system, and the microwave stability threshold during this dynamic regime.

4.1 γ_{tr}-jump Lattice Design

Previous optical design principles of the γ_{tr}-jump schemes have been presented in detail by T. Risselada [13]. Additional quadrupoles are added to the lattice to change the dispersion function through the dipoles so as to provide a, preferably linear, dependence of γ_{tr} on quad excitation. At the same time it is desirable that the betatron functions and the tunes of the accelerator should be unchanged. The condition for constant tunes is :

$$\Delta\nu_x = \frac{1}{4\pi}\sum b_i K_i = 0 \tag{4.1}$$

where K_i is the perturbation strength.

If, in addition, a doublet pair of γ_{tr}-jump quadrupoles has a betatron phase difference of $n\pi/2$, then it does not produce an external betatron wave. A major problem though for all γ_{tr}-jumps is that the maximum value of the dispersion function is difficult to control [14]

The design goal for the RHIC γ_{tr}-jump was the desire to maintain a physically small beam size during the jump to minimize the possibility of beam loss and subsequent magnet quenching while providing the necessary jump parameters. The limits on the maxima of the dispersion function were set to keep the actual beam size during the transition within the same limits as during injection. With an estimated peak momentum spread of 0.2% then a dispersion value of 2.5m satisfies this beam size requirement.

The *RHIC* γ_{tr}-jump was designed with two different quadrupole circuits controlling γ_{tr} and $\Delta\nu_x$ independently. With the relation ship between the quad strength and the γ_{tr} change, provided by Risselada as:

$$\Delta(1/\gamma_{tr}^2) = \Delta(dC/d\delta) = -\sum K_i Di^* Di \tag{4.2}$$

where D_i^* and D_i are the dispersion functions at the location of the additional quadrupoles when the jump is "on" and under the regular conditions, respectively. The maximum value of the function $\Delta(1/\gamma_{tr}^2)$ are obtained where the D_i^2 has maximum. This condition shows that the best positions for the γ_{tr}-jump quadrupole doublets are at horizontal dispersion maxima. This design satisfies this condition. Other sets of quadrupole doublets are used at the locations, within the straight section, where the dispersion was very close to zero. These groups do not affect the value of γ_{tr}; they are used to control the tunes. There are two doublets per interaction region where the dispersion has maximum values and an additional two doublets at locations where the dispersion is close to zero. The betatron phase differences between each group of doublets are close to π which makes them "local". The total number of the additional γ_{tr} quadrupoles per ring in *RHIC* is 48. The required change of $\Delta\gamma_{tr} = 0.8$ was obtained with a bi-directional γ_{tr} change of $\Delta\gamma_{tr} = \pm 0.4$. The quadrupoles used for the jump are standard correction package devices operating at a 25A level. The jump scheme is described in detail in [15]. The perturbed lattice ($\Delta\gamma_{tr} = 0.4$) is shown in Figure 4.2. The γ_{tr}-jump is well matched to the unperturbed lattice functions with the beta and dispersion maxima some 20% greater then the standard values.

4.2 Beam Loading Considerations

Tracking studies carried out by Wei [12] and repeated by Deng [16] have shown that the beam blow-up in longitudinal phase space depends critically on the parasitic rf voltage induced in the supposedly inactive cavities of the storage system. Both calculations show that a purely sinusoidal voltage of 10kV on the storage cavities leads to a blow-up of 10%, and this value has been chosen as the design limit. The shape and magnitude of the actual beam induced voltage has been evaluated by Ratti [17] for the scheme of two individual cavities per ring combined with six common cavities in the interaction region. The voltage seen by a beam of infinitesimally short bunches consists of two components:- a) A self induced part (immediate response) that is (in a first approximation) given by: n x q/C, where n is the number of cavities, q the charge of an individual bunch, and C the equivalent capacitance of a single cavity. This voltage component starts at zero and ramps linearly during the beam passage up to the full amplitude which depends only on the number and geometry of the resonators. The calculated value is 8 x 3.4kV at nominal bunch parameters and it is phase inductive (in quadrature with the beam).

b) A remnant part (the long range wake) that is the buildup of all the decaying response of the beam that passed during the memory of the cavity. This part is in phase with the beam. The voltage is approximately

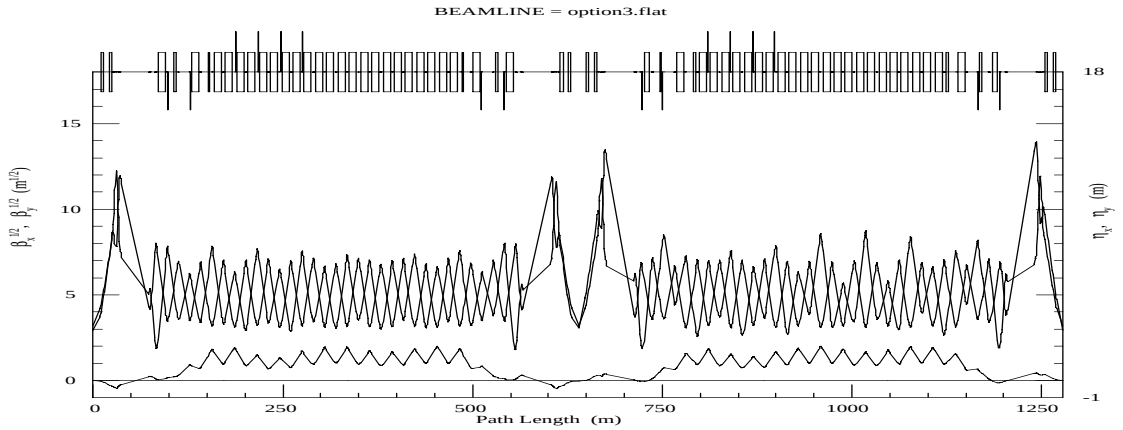

Figure 4.2: Perturbed lattice functions for $\Delta\gamma_t = 0.4$ units.

constant during the beam passage, its' magnitude inversely proportional to the cavity Q. It can thus be reduced by passive damping (de-Qing) of the resonators or by active rf feedback.

The performance of rf feedback is limited by the maximum available correcting power of the final amplifiers. Passive de-Qing of the cavities by the existing damping loops permits a larger reduction of induced voltage for the RHIC storage cavities. Nevertheless, the remnant voltage is still as high as 24kV if the beams cross at the interaction point such that their response is additive for the cavities. A method to reduce the coherent addition of the induced voltage has been proposed by Brennan [18]. The beams in the two rings are phased at transition such that their cavity responses subtract rather than add, leading to a remnant voltage of only 8kV. This scheme, made possible by the fact that the beams do not need to collide at transition energy, is certainly applicable for equal and unequal ion species; further studies are necessary to investigate ions and protons.

Further studies are also needed to confirm the permissible limit of beam induced voltage considering different rf phases and waveforms. For longer bunches approaching the rf wavelength the self induced voltage change phase gradually such that the above mentioned distinction between self-induced and remnant fields vanishes. This implies a refinement to the tracking code to simulate a cavity-beam interaction rather than a single sided beam reaction to a supposedly constant cavity voltage. Sensitivity to parasitic beam loading in the storage system is a major factor in defining the maximum cavity voltage of 300 kV for the accelerating system.

4.3 Hardware Implications

As indicated in the previous section, passive de-Qing of the storage cavities is the preferred method for minimum beam induced voltage; this implies that adequate time has to be reserved during the cycle to actuate the damping loop. The existing loops with the original drive mechanism can be moved within a fraction of a second at the price of reduced reliability in the mechanical drive bellows. Withdrawal within a few seconds is considered entirely reliable. Loop insertion can be performed at any time before injection. Loop withdrawal in presently conceived to take place during the preparation phase for the beam hand-off when the bunches are long and hence their spectral component at storage frequency is low.

The accelerating cavities must be able to change phase by 180 degrees during transition. Tracking studies have shown that 100msec is an acceptable time for this phase flip to occur though this value can be prolonged with little consequence. The accelerating voltage should be kept high, 400kV, during this time to minimize the effect of the parasitic voltage at the storage cavities. The dynamic properties of the accelerating system [18] do allow such rapid gymnastics thanks to the local rf feedback and a driver chain with sufficient peak power to make full use of the very large reserve in current rating of the final amplifier.

4.4 Microwave Stability at Transition Energy

Near the transition energy, the frequency spread which provides Landau damping diminishes along with the vanishing phase stability and small synchrotron oscillation frequency. Both the reactive and resistive components of the broad band impedance are likely to induce an instability. The threshold for microwave instability to occur at transition is [11] for a parabolic bunch distribution

where is the peak rf voltage, is the synchronous phase, $\frac{Z}{n}$ refers to the broadband coupling impedance at the microwave frequency range, is the peak current at transition, and is the maximum phase spread of the bunch at transition. During transition as the bunch length shortens then the peak current rises and the

phase spread of the bunch decreases. Both effects result in a lowering of the $\frac{Z}{n}$ threshold. In the absence of a γ_{tr}-jump, the threshold impedance is 1.4Ω for a bunch of 10^9 gold ions.

With a γ_{tr}-jump of 0.8 units within a time period of 60ms, the rate at which the beam crosses the transition energy becomes 9 times faster. The instability threshold is determined by the bunch configuration immediately before and after the γ_{tr}-jump [12] since the bunch is effectively stable during the jump time. Under these conditions the threshold impedance rises to 3.0Ω, as compared to the machine impedance estimate of 2Ω at these frequencies.

Chapter 5

REBUCKETING

The main issues are

- how to shorten the bunches
- how dangerous the microwave instability is
- beam loss

The ultimate task of the *RF* systems is to put the bunches in storage cavities, with as little beam loss as possible, for physics experiments. The longitudinal emittance determines how difficult it is to make such a "handoff" between accelerating cavities and storage cavities.

Rebucketing describes the process of moving the beam from accelerating system to storage system. The storage system provides approximately $\tau^s_{bkt} = 5ns$ bucket length, therefore given a margin of 80% for safety, the bunches have to be shorter than $\tau^s_{bun,m} = 4ns$ in order for the storage system to rebucket them (the bunch length is defined as containing 95% of the particles in a bunch.). Away from transition region in which the bunch is naturally short, the bunch length can be shortened (lengthened) by manipulating the bucket height or the bucket phase relative to the bunch center.

Since the bunch length is inversely proportional to $V^{\frac{1}{4}}$, the adiabatic compression of bunch length has a quartic power law for the voltage required. For instance, a bunch is $6ns$ long at voltage of $300kV$, to compress it down to $4ns$, the voltage has to increase to $300 * (\frac{6}{4})^4 = 1.5MV$, which is excessive in comparison with the maximum available volts from accelerating cavities.

Other ways to compress the bunch length is by non-adiabatic changes, fast than the synchrotron period.

5.1 Bunch Rotation

The *RHIC* design manual calls upon bunch rotation to shorten the bunch length with stationary buckets (see Figure 5.1). The gap voltage on the accelerating system is adiabatically lowered from nominal accelerating voltage $V^a_a = 300kV$ to a nominal shortening voltage V^a_l to compress the momentum spread within the bunch and thus lengthen the bunch length, then is snapped back on again in a time scale much shorter than a synchrotron period (approximately $40ms$ for gold at top energy.). The bunch no longer matched to the bucket starts to rotate as a whole in the synchrotron phase space, after a quarter of synchrotron period, the bunch length reaches its minimum. At that point, the accelerating cavities is turned off, the storage system is turned on in a time scale much shorter than a synchrotron period at V^s_m to rebucket the bunches.

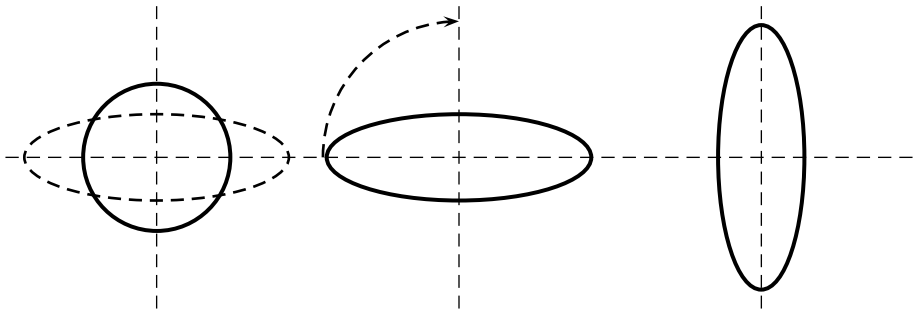

Figure 5.1: Bunch rotation. Bucket not shown.

Nominal shortening voltages in accelerating system and nominal matching voltages in the storage system for gold beam and proton beam are listed in Table 5.1. In addition to top energy, the point at which the bunch length is maximized after transition is also considered in the table.

γ	39.5	108	268
$\tau^a_{au}(ns)$	7.6	6.5	
$V^a_{au,l}(kV)$	25	45	
$V^s_{au,m}(kV)$	900	480	
$\lvert\frac{Z}{n}\rvert_{au}(\Omega)$	8	6	
$\tau^a_p(ns)$	6.0	5.1	4.1
$V^a_{p,l}(kV)$	60	115	300
$V^s_{p,m}(kV)$	350	185	70
$\lvert\frac{Z}{n}\rvert_p(\Omega)$	4	3	2

Table 5.1: Nominal shortening voltages in accelerating system and nominal matching voltages in the storage system. $\epsilon = 0.3eVs/u$. Bunch lengthes before rebucketing are also listed.

Injection and transition crossing are two major regions for longitudinal emittance blowup. So far we have assumed that the emittance stays constant from injection up to rebucketing. Table 5.2 lists some major parameters where the longitudinal emittance is $0.4eVs/u$, that is a 30% blowup is assumed.

5.2 Bunch Shortening by Unstable Fixed Point

Another way to reduce the bunch length is to shift the stable and unstable fixed point of the bucket back and forth to the bunch center (see Figure 5.2). After a fractional of synchrotron period the bunch has elongated along the separatrix of the bucket, shift the stable fixed point back to the bunch center again. The bunch

γ	39.5	108	268
$\tau^a_{au}(ns)$	8.8	7.5	
$V^a_{au,l}(kV)$	15	25	
$V^s_{au,m}(kV)$	1600	850	
$\lvert\frac{Z}{n}\rvert_{au}(\Omega)$	12	8	
$\tau^a_p(ns)$	7.0	5.9	4.8
$V^a_{p,l}(kV)$	35	65	150
$V^s_{p,m}(kV)$	650	330	145
$\lvert\frac{Z}{n}\rvert_p(\Omega)$	6	4	3

Table 5.2: Nominal shortening voltages in accelerating system and nominal matching voltages in the storage system. $\epsilon = 0.4eVs/u$. Bunch lengthes before rebucketing are also listed.

being unmatched starts to rotate in the phase space, unlike the previous case, the bunch has to rotate 3/8 of a synchrotron period to reach its minimum bunch length position. This method is faster comparing with bunch rotation. For example, to shorten the bunch by a factor of 2, the time the bunch has to sit at the unstable fixed point is $\frac{\ln 2}{2\pi} \approx 0.1$ synchrotron periods, the whole process takes about half of a synchrotron period ($\frac{3}{8}+0.1$), or $20ms$ for gold beam at top energy. If there is a phase error in the process, it will introduce a dipole motion for all the bunches, which is then taken care of by beam control system.

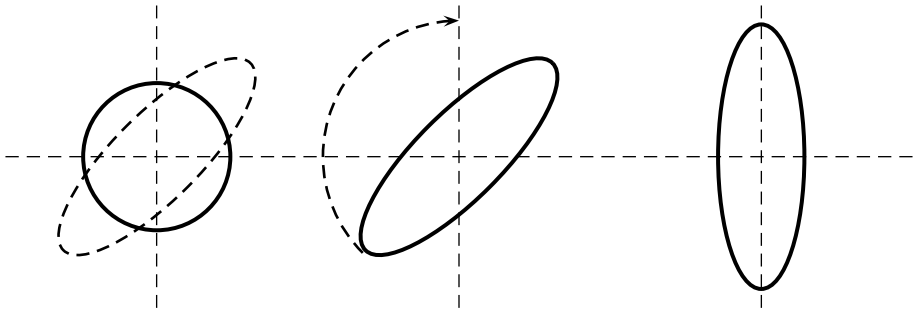

Figure 5.2: Phase jump back and forth between unstable and stable fixed point. Bucket not shown.

5.3 Microwave Instability

A potential problem with the bunch rotation method is the danger of microwave instability. As the voltage is reduced, the momentum spread in the bunch is reduced, so is the threshold of the instability. To make matters worse, the adiabaticity demands the duration of lowering the voltages in a few synchrotron periods

$e.g.5$, thus exposing the beam a long time to microwave instability. At top energy for gold beam, the total time is about $210ms$ ($5 + \frac{1}{4}$ synchrotron periods.) to finish the process.

Apply Keil-Schnell criterion to bunched beam, we have

$$\left|\frac{Z}{n}\right| \leq F \frac{m_0 c^2 \beta\gamma \mid \eta \mid}{e} \left(\frac{(\frac{\Delta P}{P})^2}{I_0}\right)_{inst} \tag{5.1}$$

$\frac{\Delta P}{P}$ is taken at full spread at half height, F is a form factor of order of 1. Suppose the distribution in both the energy and the phase is square of cosine function. Then for a bunch whose length is τ and total charge is Q. The above equation reads as

$$\left|\frac{Z}{n}\right| \leq \frac{V_{rf}\tau[1 - \cos(\omega_{rf}\tau/2)]}{2\pi h Q} \tag{5.2}$$

Some limiting values are listed in Tables 5.1, 5.2.

It is being estimated that the broad band impedance $|\frac{Z}{n}|$ in $RHIC$ is in the order of $2\,\Omega$, it seems that the dangerous spot in for proton beam at top energy.

5.4 Beam Loss

Suppose the storage cavities are turned on when the bunches reach their minimum lengths, the beam spilling out of the storage bucket happens when the height of the storage bucket is smaller than the momentum spread within the bunch. It is thus expected the beam loss to be negligible if the storage cavities deliver enough voltage, see Table 5.1 5.2.

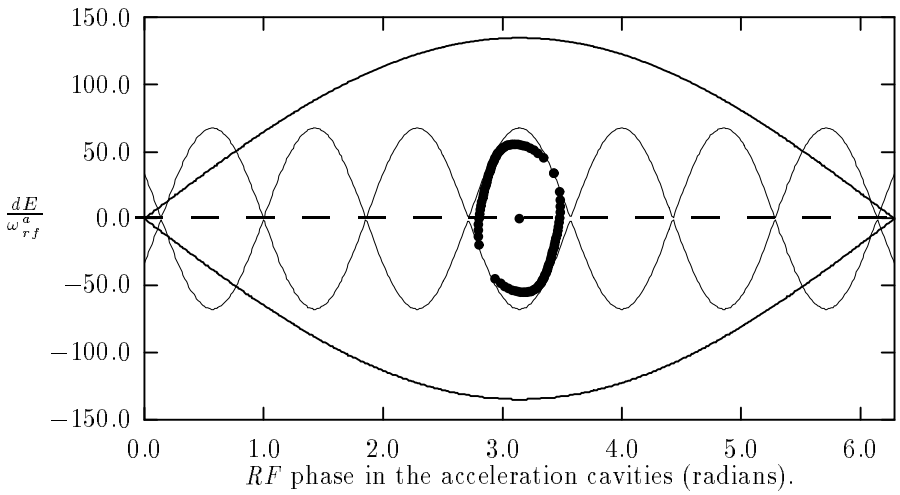

Figure 5.3: Dashed line is the bucket in 26MHz bucket, solid line is the storage bucket, dots are representative particles. $\epsilon = 0.3\,eVs/u, V^a_{rf,a} = 300\,kV, V^s_{rf,s} = 550\,kV$

It's simulated for gold beam at top energy in two cases, one is at emittance of $0.3\,eVs/u$ and the other at $0.4\,eVs/u$ to illustrate the situation when the bunch has rotated to the right orientation and the storage system is turned on, see Figure 5.3 5.4. The contour of particles occupy in the phase space of $0.3\,eVs/u$

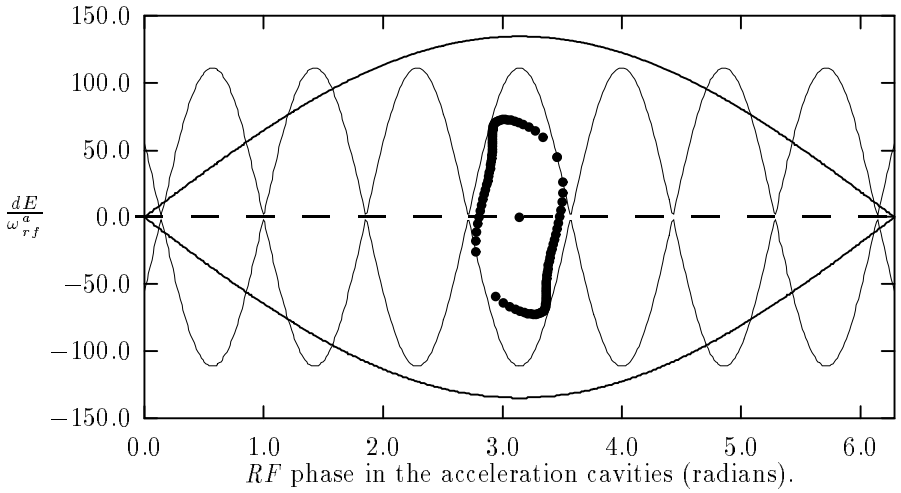

Figure 5.4: Dashed line is the bucket in 26MHz bucket, solid line is the storage bucket, dots are representative particles. $\epsilon = 0.4\,eVs/u, V^a_{rf,a} = 300\,kV, V^s_{rf,s} = 1500\,kV$

and $0.4\,eVs/u$. respectively. The distortion on the bunch shape indicate that part of the bunch is inside of the nonlinear region of the RF bucket in the accelerating cavities. The distortion gets worse for the case of $0.4\,eVs/u$, the matching voltage increases significantly from the nominal values listed in Table 5.2.

For a beam lossless "transfer" from accelerating cavities into storage cavities, it is important to begin with small longitudinal emittance. If the beam has to be held initially by two storage cavities in each ring, the longitudinal emittance should be kept no more than $0.4\,eVs/u$ at the end of acceleration to the top energy.

5.5 Conclusion

The bunch shortening at the unstable fixed point is much faster than the synchrotron period, with the microwave instability threshold significant higher than for the adiabatic bunch compression scheme. It further avoids the complications of running accelerating cavities at low gap volts. This is the technique which has been chosen for the baseline design. The longitudinal emittance should be kept below $0.4eVs/u$ to avoid potential beam loss situations and a specification of $0.35eVs/u$ has been adopted. Under this scenario the beam appears to be stable for all particle species.

Chapter 6

STORAGE

After having reached the collision energy, both proton and heavy ion beams are transferred from the acceleration to the storage rf system at 196 MHz. For Au ion beam, the operating energy is from 30 to 100 GeV/u. For other ions of charge state Z and atomic mass number A, the maximum operating energy is 250 Z/A GeV/u.

The choice of the storage rf frequency is based upon several competing factors. In order to fulfill the experimental requirements on short bunch length, the rf frequency should be higher than 160 MHz so that the maximum bunch length after the growth due to intra-beam scattering is less than about 31 cm. On the other hand, with a frequency much higher than 200 MHz, the rf voltage needed to provide adequate momentum aperture to accommodate for the IBS emittance growth is high and costly. Since the CERN SWC cavities to be adapted for use in RHIC typically operate at 200.1 MHz, it is straightforward from hardware point of view to choose 196 MHz as the operation frequency for RHIC storage. This frequency corresponds to a harmonic number of $h = 22 \times 2 \times 57 = 2508$. It thus allows the possible future upgrade of doubling the number of bunches in each ring from 57 to 114.

6.1 Intra-beam Scattering

During storage, the luminosity deterioration due to beam loss and growth caused by intra-beam scattering is of primary concern. Particles in the same bunch exchange longitudinal and transverse momenta by Coulomb scattering. The scattering cross section is proportional to Z^4/A^2, hence the effect is particularly severe for high-Z ions like Au. Compared with that of a proton bunch of 10^{11} particles, the effect of IBS on the Au beam is one order of magnitude stronger even though each bunch includes only 10^9 particles.

Except for a form factor that depends on the lattice parameters, the beam energy, and the relative spreads in velocity, the diffusion rate caused by IBS is linearly proportional to the particle density in the 6-dimensional phase space. As an order-of-magnitude estimate, assume that the distribution of the N particles in the bunch is Gaussian in phase space, and the transverse motion is fully coupled. When the beam is stored at energies much higher than the transition energy γ_T of the machine, the relative growth rates of the transverse and momentum spreads are [19] approximately:

$$\begin{bmatrix} \frac{1}{\sigma_p} & \frac{d\sigma_p}{dt} \\ \frac{1}{\sigma_{x,y}} & \frac{d\sigma_{x,y}}{dt} \end{bmatrix} = \frac{C_0 Z^4 N}{A^2 \beta^4 \gamma_T} \frac{1}{\epsilon_{Nx}\epsilon_{Ny} S} \begin{bmatrix} (1-d^2)/d \\ d/2 \end{bmatrix}$$

where D_p is the average dispersion, $d = D_p\sigma_p/(\sigma_x^2 + D_p^2\sigma_p^2)^{1/2}$ is typically of order 1, $C_0 = 13.5\pi L_c m_0 c^2$, ϵ_{Nx} and ϵ_{Ny} are the normalized 95% transverse emittances, S is the 95% longitudinal bunch area, and βc is

the particle velocity. The Coulomb scattering logarithm, L_c, is estimated to be 20.

The detailed IBS calculation is based on a model applicable to RHIC operation. The beam loss in transverse direction is assumed to be negligible before the transverse emittance ϵ_N exceeds about 40π mm·mr. The transverse distribution, though time dependent, is Gaussian during the entire storage period. The horizontal and vertical motions are fully coupled within time periods much shorter than the IBS diffusion time [20]. Results are qualitatively similar when the degree of coupling is reduced. The growth rates are averaged over the entire circumference of the ring. The actual variations of the lattice functions have been taken into account.

The evolution of the beam during the storage period is evaluated by iteration processes. Initially, a bunch of 10^9 Au ions is assumed to be transferred into the storage rf system with transverse emittances ϵ_N of 10π mm·mr and bunch area of $0.3eVs/u$. The evolution of longitudinal distribution is obtained using the Fokker-Planck approach [21]. Particles are assumed to be lost when they reach the rf separatrix. At each iteration step, the beam intensity is adjusted according to the longitudinal beam loss, and the transverse rms beam sizes are adjusted according to the growth rates.

With a peak rf voltage of 6 MV, the bunch longitudinally fills the bucket in less than 1 hour. The rms bunch length increases to about 22 cm. Afterwards, the longitudinal beam dimension remains unchanged, while the beam loss occurs through the rf separatrix. At the end of the 10 hour storage, the total beam loss is near 40from 10π to about 40π mm·mr.

Fig 6.1 shows the 10 hour beam survival rate and average luminosity as functions of the peak voltage of the storage rf system. The β^* at the crossing point is assumed to be 1m. Beam loss due to nuclear processes and transverse aperture limitation are not taken into account. With low rf voltage, the luminosity is severely limited by the IBS beam loss. With increased rf voltage, more particles survive during the storage. On the other hand, the transverse beam sizes grow to larger values due to these additional surviving particles which potentially introduces transverse dynamic aperture lifetime limitations as well as limiting the luminosity gain. The resulting average luminosity improvement is determined by these two competing factors.

With the 1m β^* operation, the transverse physical beam size is large at the triplets where $\beta_{x,y}$ reach about 1400m. Transverse beam loss is expected to occur when ϵ_N exceeds about 40πmm·mr. From the point of view of the average luminosity, the optimum voltage lies within a range of 6 to 10 MV. The layout chosen has an effective 8 cavities per ring for a maximum voltage of $\sim$ 8MV. Further luminosity improvement can be achieved when transverse and longitudinal stochastic cooling are applied to the stored beams.

6.2 RF Noise

The noise from the rf system induces diffusion in the beam. In the case of beam storage in RHIC, the rf bucket is full during most of the period. In addition to the intra-beam scattering, rf noise also results in beam growth and beam loss in longitudinal direction. Because of the non-linear synchrotron motion, noises at odd integral multiples of the synchrotron-oscillation frequency contribute to beam diffusion.

From the experience of the CERN SPS operation [22], rf noise is mainly contributed from the low-lever rf control (frequency or phase modulation) and possible high-voltage ripple. Suppose that in the critical frequency range the phase discriminator noise in the feedback loop dominates [23]. In order for the noise induced beam intensity reduction to be within a tolerable value of 2% per hour, which corresponds to a life-time of about 50 hours, the phase noise level must be lower than 5×10^{-6} rad/$\sqrt{\text{Hz}}$. This noise level is about three times that achieved with the CERN SPS rf system (1.6×10^{-6} rad/$\sqrt{\text{Hz}}$).

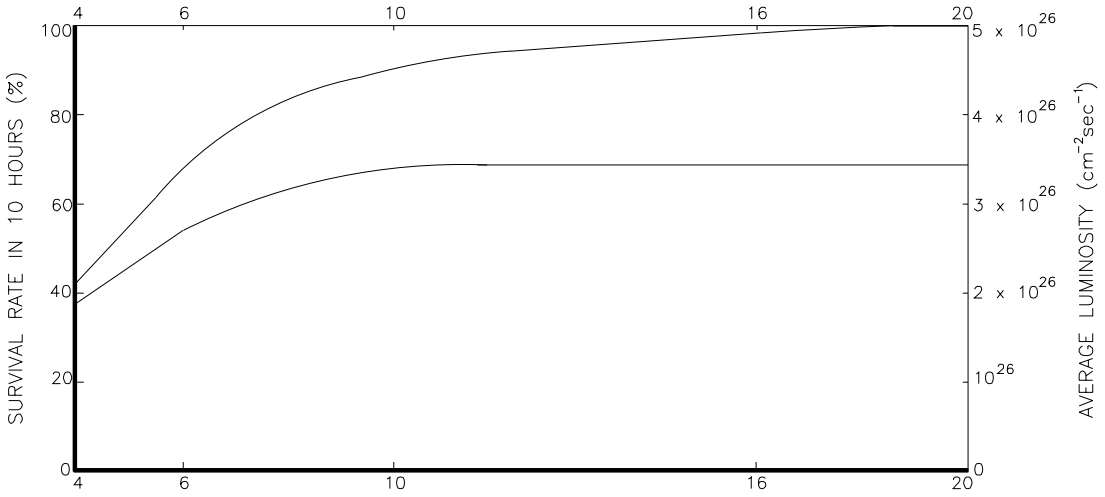

Figure 6.1: Dependence of final beam survival rate and average luminosity on storage rf voltage after 10-hour operation, "constant voltage" scenario.

6.3 Beam Loading

In order to accommodate for the beam growth caused by intra-beam scattering, a total of at least 6 MV gap voltage is required. Compared with other operation cycles, this large gap voltage makes the effect of beam loading less significant during the storage [24].

Beam loading in the RHIC storage cycle is characterized by the periodic transients due to the missing bunches and the steady state compensation. During the normal operation, the gap in the bunch train given by the four missing bunches lasts for about 1 μs. Assume that the beam in each ring consists of 57 bunches, and that the beam loading from each beam adds up linearly in amplitude in the cavity then the phase shift induced by this gap is given by:

$$\Delta\phi = \frac{1}{2}\frac{R}{Q}\frac{\omega_{rf}}{V_g} I_b \Delta t = 1.47 \text{ deg}$$

where $R/Q = 167$ Ohms, $V_g = 800$ kV is the gap voltage, $\Delta t = 1\mu$s, and the peak current in each beam is about 0.1 Amp. Such a phase shift is at the limit of sensitivity of the phase detector. It corresponds to a longitudinal drift of the interaction point of about 6 mm.

It is proposed that the gaps in the beams circulating in the different ring are phased such that they will cross the rf cavity region simultaneously. This will further minimize the beam loading. Therefore, compared with the effect of intra-beam scattering, the effect of beam loading is insignificant.

6.4 Instabilities

Due to its relatively high beam intensity, the proton beam is, among different species of ions, most vulnerable to instabilities. At the storage energy of 250 GeV, the threshold impedance (Z/n) for microwave instability is about 10 Ohms for the proton beam.

Calculation of longitudinal coupled bunch instability thresholds and growth rates have been undertaken for both proton and gold beam. The impedance assumed consisted of the rf cavity modes, space charge (negligibly small at storage), and a broadband component due to bellows etc. (Z/n=-i2 Ohms). Both gold and proton beam appear to be Landau damped and stable during the storage.

6.5 RF Gymnastics and Interaction Point Scanning

The only kind of beam gymnastics considered so far is the removal of particles outside of the bucket which may impair detector operation. Further studies are necessary to determine details of the operation, but it is expected to involved small amounts of acceleration/ deceleration requiring the modulation of voltage and frequency of the storage rf system. The limiting factor will be the slew rate of the bending magnetic field rather than the agility of the cavities. This is valid as long as these gymnastics don't involve the common cavities (i.e. for zero voltage at these units or for synchronous operations in both rings with stationary interaction point).

Scanning of the interaction point breaks the rf symmetry between the two rings [25]. From the point of view of the common cavities the lack of symmetry is not critical since the composite beam load decreases in magnitude and remains always reactive. The two beams are however treated differently,. one crossing each cavity gap with accelerating voltages, the other with decelerating voltages. The resulting difference in kinetic energy has to be compensated for by the individual cavities of each ring; due to their voltage limit the extent of interaction point scanning is thus restricted to $\pm$60mm. On top of this comes the amplifier limit for the provision of additional beam power, which constrains the duration of a scan to 200 msec within each 1 sec interval.

The extent and duty cycle of the scan may be increased by putting more individual cavities in each ring and reducing the number of common units in the interaction region. This will facilitate the beam transfer process as well as the phase synchronization of the two rings, but reduce the overall available rf voltage. More studies are necessary to devise the optimum compromise.

Chapter 7

OPERATING CYCLE

A baseline rf cycle for gold is presented to meet the requirements imposed by the preceding sections. The rf cycle is depicted in the following Figures 7.1- 7.6, showing as a function of time $\frac{dB}{dt}$, rf voltage, rf frequency, γ_{tr} and γ_s, synchrotron frequency and the bucket and bunch lengths. The magnetic field is assumed to have a constant of $\frac{dB}{dt}$ 500 Gauss/sec. The rf voltage is set to 170 kV providing stationary matched buckets to the bunches injected from AGS. It is then ramped up to the accelerating voltage of 300 kV and kept constant as the beam crosses transition via the γ_{tr} jump. At this point in the rf cycle the synchrotron frequency has dropped to approximately 16 Hz and begins to rise. if the rf voltage was to be held at 300 kV the synchrotron frequency would rise to 35 Hz and then slowly cross through 30 Hz, and the bunch would become susceptible to resonances from coupling to the power line harmonics. The voltage is therefore reduced back down to 170 kV to keep the synchrotron frequency safely below 30 Hz. The voltage is then raised to 300 kV just prior to the shifting of the stable-unstable phase point to provide the bunch shortening necessary for the rebucketing into the 196 MHz system. The shortened bunch is then captured in the 196 MHz buckets created by the 2 independent systems per ring to allow separate control of the two rings.

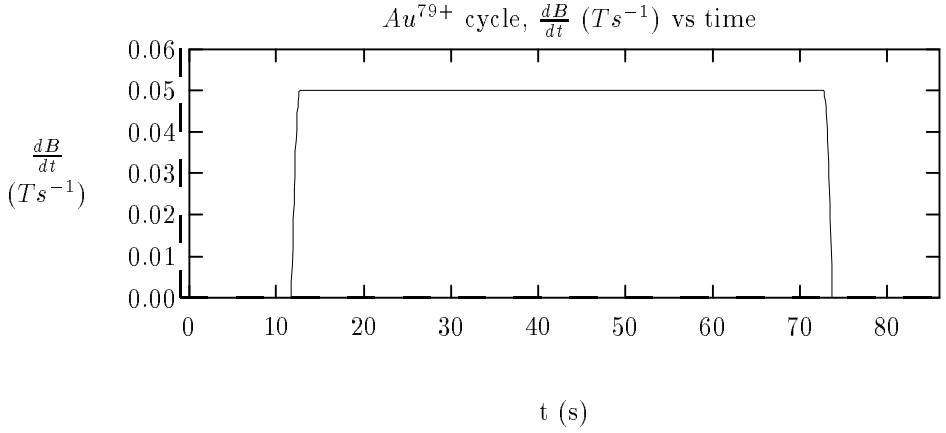

Figure 7.1: $\frac{dB}{dt}$ program.

The emittance growth for gold through the cycle is given in Tables 7.1 and 7.2, for two initial values of the emittance at injection from AGS. Injection of $0.2eVs/u$ bunch results in emittances at rebucketing of $0.35eVs/u$ and $0.34eVs/u$ for the 1st and 57th bunches respectively. These values with their small spread

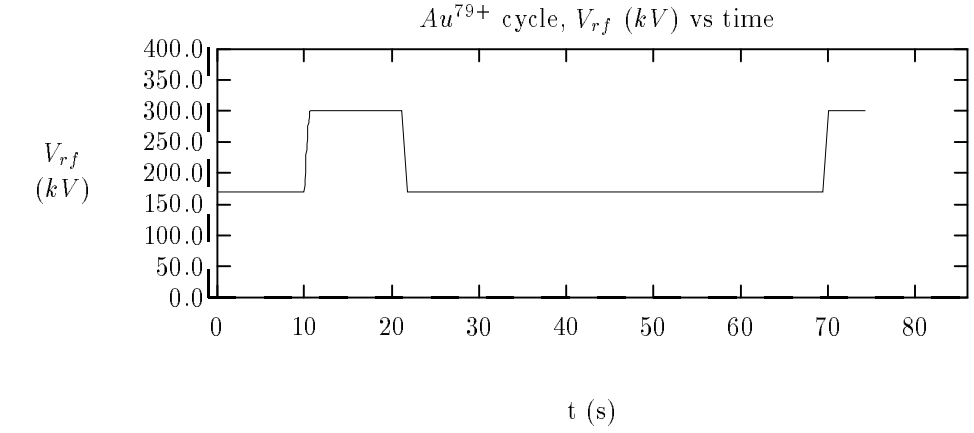

Figure 7.2: rf gap volt program.

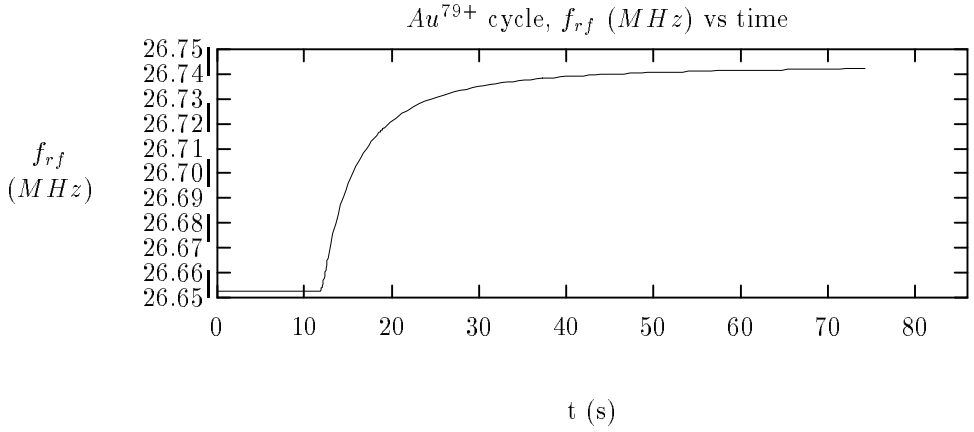

Figure 7.3: rf frequency program.

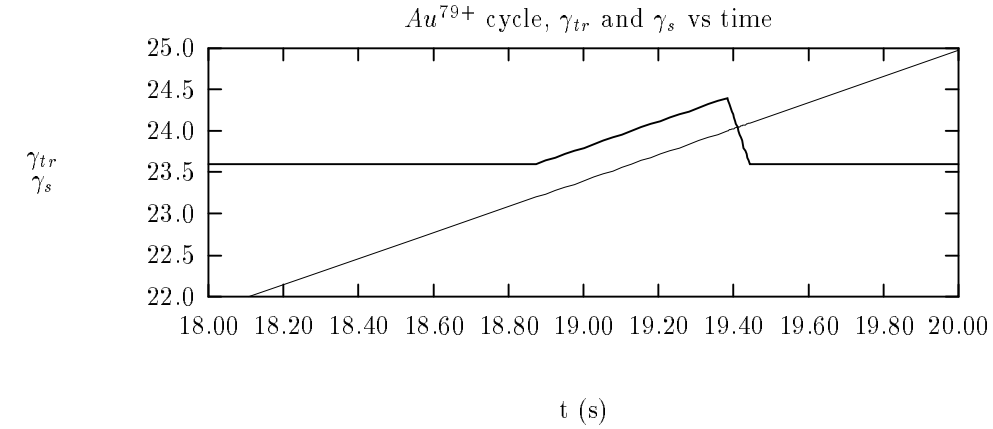

Figure 7.4: γ_{tr} jump region.

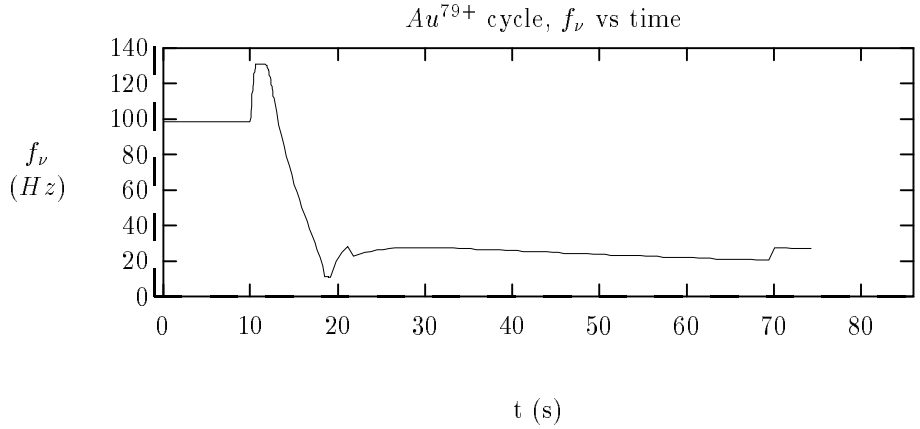

Figure 7.5: Synchrotron frequency in the cycle, notice it never crosses 30 Hz line.

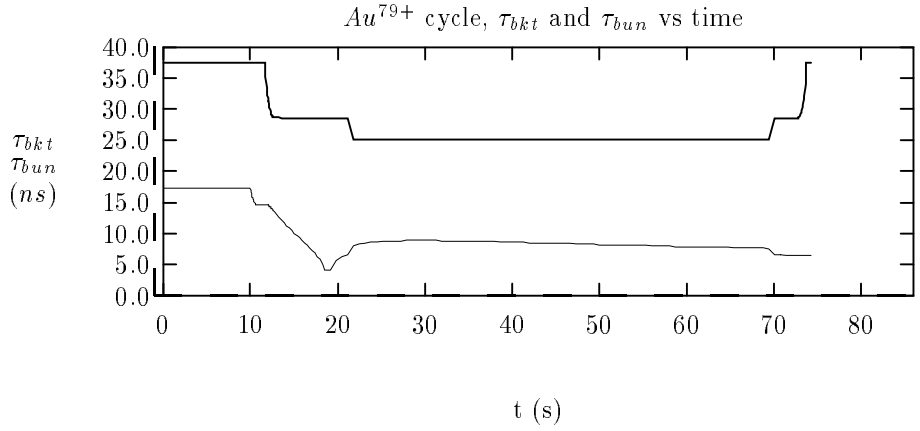

Figure 7.6: Bunch and bucket lengths variation throughout the cycle.

allow rebucketing with minimum beam loss. Emittance growth for initial values of $0.3eVs/u$ injected bunches leads to $0.46eVs/u$ and $0.39eVs/u$ for the 1st and 57th bunch which could in turn lead to unacceptable beam loss during rebucketing.

Bunches	1st	57th	
At injection	0.2	0.2	from AGS
	0.22	0.22	injection error dilution (10%)
	0.26	0.22	IBS blowup (20% for the 1st, and 0 for the 57th)
At transition	0.26	0.22	assuming no dilution during acceleration
	0.32	0.31	space-charge and nonlinear effects (20% for the 1st, and 40% for the 57th)
	0.35	0.34	remnant voltage from storage cavities (10%)
At rebucketing	0.35	0.34	

Table 7.1: Estimates of evolution of longitudinal emittances (eVs/u).

Bunches	1st	57th	
At injection	0.3	0.3	from AGS
	0.33	0.33	injection error dilution (10%)
	0.38	0.33	IBS blowup (20% for the 1st, and 0 for the 57th)
At transition	0.38	0.33	assuming no dilution during acceleration
	0.42	0.35	space-charge and nonlinear effects (20% for the 1st, and 40% for the 57th)
	0.46	0.39	remnant voltage from storage cavities (10%)
At rebucketing	0.46	0.39	

Table 7.2: Estimates of evolution of longitudinal emittances (eVs/u).

Because the proton beam is not susceptible to IBS at injection and does not cross transition, the RF cycle is straight forward. The only major contribution to emittance growth prior to rebucketing is the emittance dilution due to bunch to bunch injection errors. The estimated 10% growth of the 0.3 eV-s bunch leads to 0.33 eV-s, which is within the acceptance of the 196 MHz bucket at top energy.

7.1 The Acceleration RF Cavity and Driver System

The accelerating system consists of two 26.7 MHz cavities per ring, each with a integral power tetrode, to provide the necessary 400 kV per ring accelerating voltage.

A preliminary design shown in Fig 7.7 consists of a capacitively loaded coaxial line with a 4CW150000 EIMAC tetrode close coupled (≈20:1) to the coaxial capacitance at the high voltage end. The integral disk at the low voltage end of the cavity provides a low inductance path for attaching external ferrite tuners, which will be explored in the R&D phase to provide the necessary 1% tuning range.

The theoretical shunt impedance is 0.93 MΩ with a Q of 13587 which, when derated 30% to 0.651 MΩ and Q = 9511, leads to a dissipation of 30.7 kW at 200 kV. When combined with the 2.654 kW beam power, this yields a modest 33.35 kW. Since the power tube is rated at 150 kW plate dissipation, there is

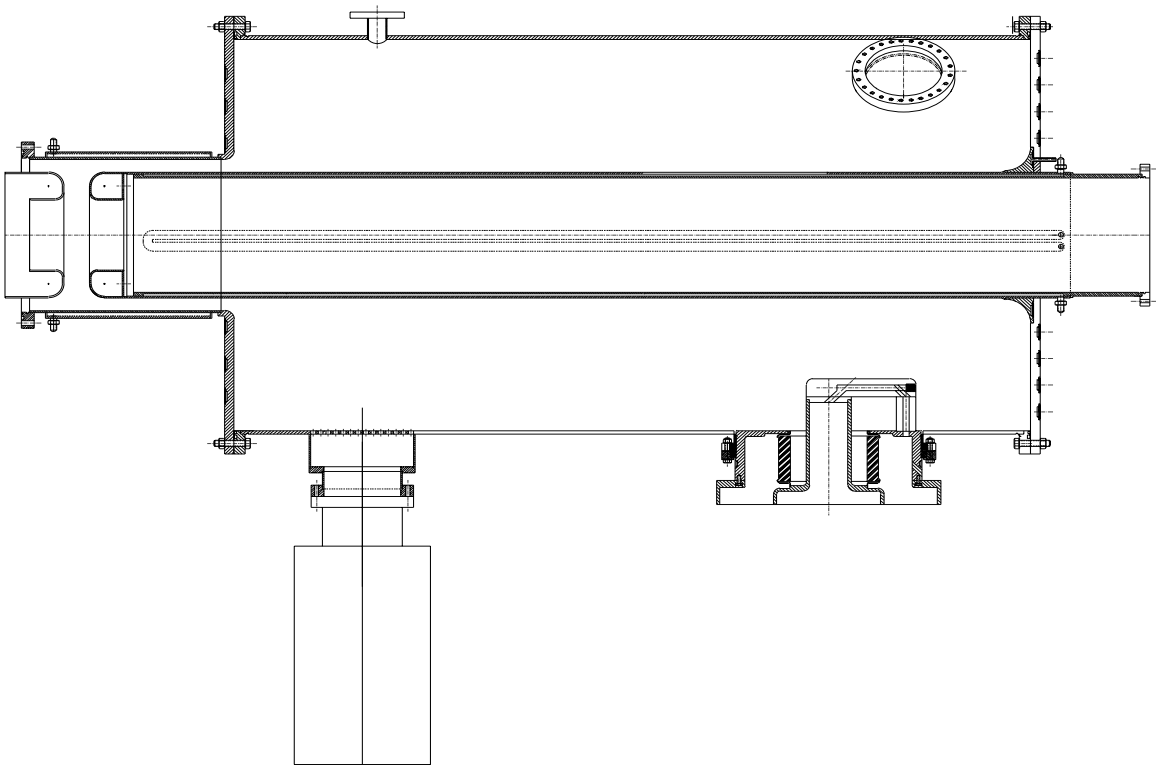

Figure 7.7: Accelerating cavity

sufficient reserve to enable any reasonable upgrades with existing components. The accelerating gap is 55 mm, providing a large safety margin on attainable gap voltage.

This preliminary design concept is being studied in detail under an R&D plan consisting of:

- Feasibility of ferrite tuner concept.
- Susceptibility of geometry (with an without coatings) to multipactoring.
- Implementation of local rf-feedback with a high gain tetrode in the final stage to reduce the beam-induced voltage during injection.

7.2 The Storage RF Cavity

Initial plans foresaw the development at BNL of a dedicated 160 MHz system. It happened, however, that CERN was introducing superconducting cavities in the SPS ring, therefore, de-commissioning part of their so-called "SWC" system working at 200.1 MHz. After a feasibility study, the decision was taken to adapt the available SWC-units for use in RHIC. Each CERN cavity is equipped with a stepping-motor driver tuner, HOM-suppressor, a pneumatically actuated damping loop to reduce the impedance of non-operating units by a factor of 500, an individual local power amplifier and the low-level circuitry. Groups of 8 cavities share a common power supply and driver. A complete description of the system may be found in the paper by P.E. Faugeras [26] an approximate view of the cavity is given in Fig 7.8.

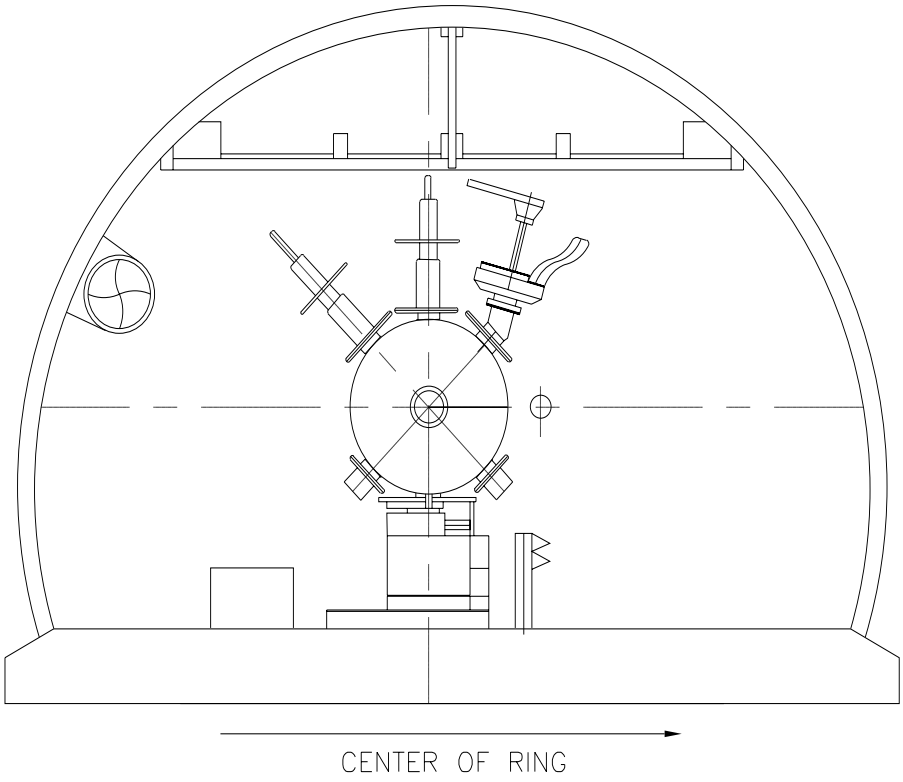

Figure 7.8: Sketch of a storage cavity and its auxiliaries in the tunnel.

The main modifications for use in RHIC include:

- returning of the system to a lower frequency by capacitive insertions in the cavity and by readjusting the power amplifier.
- addition of individual driver amplifiers to implement local rf feedback loops for reduction of the beam-induced voltage.

The modified units will possess the following parameters

Frequency (MHz)	196.1
R/Q (Ω)	162
Q (unloaded)	44000
Q (with local feedback)	250
Voltage (MV/cavity)	1

Table 7.3: Parameters of the storage cavities

7.3 The Wideband Cavity

The wideband cavity will be similar to the acceleration cavities, i.e., a 1/4 coaxial resonator with $f_{res} = 342 f_0$. However, there will be no tuning, the gap will be ceramic and directly coupled to the power source. The latter will be a wideband (10 kHz - 220 MHz) 5kW power amplifier capable of developing 700 V of pulsed 26.7 MHz signal into a 50 Ω load which will be connected across the cavity gap. For a bandwidth of $\pm 57 f_0$, which is the minimum required to control all the coupled bunch modes for 114 bunch operation, a cavity with $R/Q > 175\Omega$ is necessary.

Together with the output impedance of the amplifier, the combination cavity is then a strongly over-damped resonator ($Q \approx 1/7$ for 175 Ω) whose transient response determines how well the system operates on a bunch to bunch basis. For 114 bunch stacking the correction signal would consist of pulses of three 26.7 MHz rf cycles. It can be shown that the worst-case scenario would result in 1% of the correction signal for one bunch remaining with a following bunch, if present, passes the gap. Further reduction of the transient amplitude is possible but this can only be accomplished by actual system testing.

Since this cavity can be driven remotely by coaxial cables it can be mounted on the insertion side of Q4 where the ring separation is still $\sim$ 80 cm so that both units can be opposite each other. If 700 V is not sufficient to control injection errors then a second cavity can be added to allow push-pull excitation with two power amplifiers each driving one half of a 100 Ω gap termination.

Chapter 8

CONCLUSIONS

The ultimate challenge for the RHIC rf system will be emittance preservation during the various beam manipulations so that a loss free transfer from the accelerating to the storage system can be performed. The problem is most significant at the highest bunch intensities for the heaviest ions where emittance growth due to IBS becomes an additional concern. Beam stability does not appear to be a significant problem for the anticipated parameter regimes. The machine broadband impedance threshold of 2.0 Ω is determined by the estimated microwave stability criteria during rebucketing for protons. Coupled bunch modes driven by cavity HOM's are within the capability of a modest damping system for the few potentially unstable modes. The hardware specifications derived from the system requirements outlined in this report, are achievable using established techniques.

Critical beam manipulations requiring more detailed studies include the ability of the AGS to perform the necessary proton bunch rotations. A detailed simulation of beam loading in the accelerating cavities during transition taking into account real bunch dimensions, more realistic cavity simulations, and the possibility of cavity cancellation are also needed. The present IBS simulations assume fully coupled beams in the transverse degrees of freedom, the potential effect of uncoupled beams must be analyzed. The potential for reducing the IBS growth rate during storage by shaping the bunches was used at the SPS and will be considered for RHIC as well.

Bibliography

[1] Conceptual Design of the Relativistic Heavy Ion Collider. BNL 52195, May 1989.

[2] D. P. Deng. Parameters of an rf cycle for Au^{79+} and p. Rf-5, BNL, 1993.

[3] X. Pei. rf phase lock between RHIC & AGS during injection. Technical report, BNL, 1993.

[4] J. Xu. The required damping voltage for different damping speeds. Rf-11, BNL, 1993.

[5] D. P. Deng. Longitudinal emittance blowup during injeciton damping. Rf-12, BNL, 1993.

[6] R. Baartman. Bunched beam longitudinal stability, 1991.

[7] K. Satoh. Stability of HOM's in a bunched beam w/o mode coupling. Technical report, SLAC.

[8] Kick and Peggs Gabella, Rosenzweig. rf Voltage Modulation at Discrete Frequencies with Applications to Crystal Channeling Extraction. Technical report, FNAL, 1992.

[9] J. Rose. Preliminary design considerations for RHIC accelerating cavity tuners. Rf-9, BNL, 1993.

[10] D. P. Deng. Longitudinal emittance growth due to rf phase errors. Rf-3, BNL, 1993.

[11] J. Wei. *Longitudinal Dynamics of the Non-Adiabatic Regime on Alternating-Gradient Synchrotrons.* PhD thesis, State University of New York, Stony Brook, 1990.

[12] J. Wei. Transition Crossing in the RHIC. AD/RHIC 84, Brookhaven National Laboratory, 3 1991.

[13] T. Risselada. Design of quadrupole scheme to modify transition gamma. CAS lecture, 1990.

[14] L. Teng. Compensation of space charge mismatch at transition using the transition jump method. Technical report, FNAL, 1970.

[15] D. Trbojevic et. al. First order modification of transition energy at RHIC, 1993.

[16] D. P. Deng. Longitudinal emittance growth in the presence of transient beam loading. Rf-2, BNL, 1992.

[17] A. Ratti. technote in preparation. Technical report.

[18] J. M. Brennan. private communication.

[19] J. Wei. Evolution of a hadron beam under IBS. PAC Proc., 1993.

[20] G. Parzen. EPAC Proc., 1988.

[21] J. Wei and A. Ruggiero. . Technical report, 1990.

[22] D. Boussard. Proc. CAS, 1983.

[23] E. Raka. . Technical report.

[24] A. Ratti. to be published. Technical report.

[25] W. Pirkl. . RF-7, 1993.

[26] P.E. Faugeras et. al. The new rf system for Lepton acceleration in the CERN SPS. Proc. of PAC, 1987.